ACS APPLIED MATERIALS & INTERFACES

RESEARCH ARTICLE

www.acsami.org

Preparation of Controllable Core−Shell Gold Nanoparticles and Its Application in Detection of Silver Ions

Haowen Huang,*,† Caiting Qu,† Xuanyong Liu,‡,§ Shaowen Huang,† Zhongjian Xu,† Bo Liao,† Yonglong Zeng,† and Paul K. Chu*,§

†Key Laboratory of Theoretical Chemistry and Molecular Simulation of Ministry of Education, School of Chemistry and Chemical Engineering, Hunan University of Science and Technology, Xiangtan, 411201, China

‡Shanghai Institute of Ceramics, Chinese Academy of Science, Shanghai 200050, China

§Department of Physics & Materials Science, City University of Hong Kong, Tat Chee Avenue, Kowloon, Hong Kong, China

Supporting Information

ABSTRACT: We report a novel shell technique to prepare controllable core−shell nanoparticles. In this technique, the shell is formed when the core reacts with metal ions and $Na_2S_2O_3$ and the size of the core and thickness of the shell can be controlled. Transmission electron microscopy and X-ray diffraction reveal that the shell consists of insoluble complex salts comprising Au_2S, AuAgS, and Ag_3AuS_2. The resulting core−shell nanoparticles obtained at different reaction stages demonstrate that the formation of Au_2S, AuAgS, and Ag_3AuS_2 shell proceeds from the outside. The morphological evolution of the particles changes significantly with reaction time demonstrating that formation of the shell results from diffusion in the solid shell. The core−shell nanoparticles produced by this technique can be used as nanosensors to detect Ag^+ in aqueous media with high selectivity and sensitivity. The excellent selectivity for Ag^+ is demonstrated by comparing the response to other metal ions. In addition, our evaluation indicates that gold nanorods offer higher sensitivity than gold nanospheres.

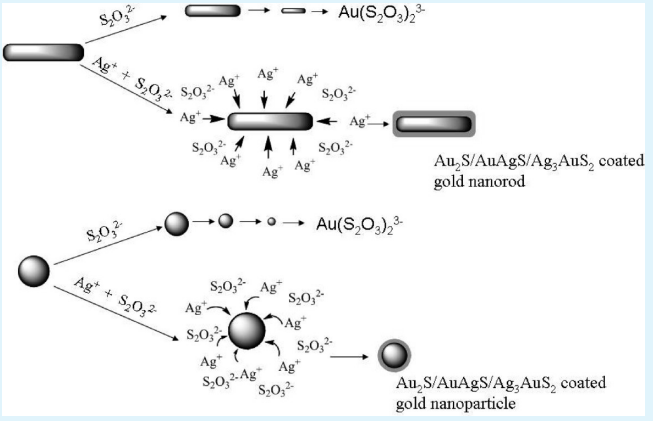

KEYWORDS: core−shell nanoparticles, gold nanoparticles, duffusion

INTRODUCTION

Currently, the fabrication of composite nanostructures using the preformed nanocrystals as building blocks is of great interests because it can integrate several different functionalities required by the applications into one common nanostructure. Attracted by the unique optoelectronic and physicochemical properties, researchers widely used core−shell gold nanoparticles in the preparation of composite nanostructures.[1,2] A useful strategy to monitor optical properties on the nanoscale involves integration of gold nanoparticles and associated localized surface plasmon into the particles or structures.

Many approaches have proven successful in tuning the localized surface plasmon resonance (LSPR) of gold nanoparticles into the near-infrared, a wavelength region of extreme technological interest to study biosensor and biotechnology. One of these approaches uses additives that alter growth rates on different facets of a metal seed, providing control of nanoparticle shape.[3] Materials obtained from these routes, notably gold nanorods, can be tuned to absorb and scatter in the near-infrared by changing their aspect ratio.[4] A second category of near-infrared active nanomaterials are produced by a stepwise process of coating one metal onto either a dielectric particle creating a nanoshell[5,6] or onto a second metal, creating a core−shell structure.[7,8] The LSPR wavelength of these nanomaterials has been tuned by altering the core size[9] and the coating thickness.[10] As a result, complex nanoparticles, particularly core−shell nanostructures, are attractive in nanobiotechnology such as the analysis of biomolecules and other target species.[11,12] The capability to detect biological molecules in vitro or in vivo with high sensitivity and selectivity in a small sample size is potentially achievable because of the distinctive electronic, optical, and magnetic properties of these nanostructures. In fact, core−shell nanoparticles have been reported to be useful in biosensing devices using fluorescent,[13] electrochemical,[14] LSPR,[15−17] and magnetic[18−20] methods.

In spite of many of composite nanostructures being fabricated by metallic and metallic compounds, which provide tremendous

Received: August 26, 2010
Accepted: December 28, 2010
Published: January 20, 2011

potential and importance to detect heavy metals for chemical, biological, and environmental reasons, there have only been few reports on the use of nanoparticles to selectively monitor metal ions,[21−23] and no report for identifying or detecting the composed metallic ions. Some analytical methods have been developed to for instance, make ratiometric fluorescent sensors for metals.[24,25] As many heavy cations are known as fluorescence quenchers, discrimination among chemically close ions is quite challenging.

Building from these ideas, we prepared Au_2S/AuAgS/Ag_3AuS_2-coated gold nanoparticles using a novel shell technique to prepare a type of controllable core−shell gold nanoparticles. There have been reported that the fabrication of the Au-coated Au_2S core−shell nanoparticles[26,27] and Ag_2S coated gold nanorods.[28,29] However, the preparation of multicomplex nanoshell is challenging. Here we synthesized a multicoplex shell coated gold nanoparticles with high yield. Moreover, the synthesized nanostructures can also provide a platform to detect trace amounts of Ag^+ in aqueous media with high selectivity and sensitivity.

In this study, the developed technique is different from many other conventional methods in that formation of the shell is the result of the core reacting with metal ions and $Na_2S_2O_3$. Not only the size of generated core−shell nanoparticles but also the core size and shell thickness can be controllable. The plasmon-derived optical resonance can be adjusted with the controllable core−shell nanoparticles. This unique red-shift of the nanoparticle plasmon resonance to wavelengths in the visible and near-infrared regions of the spectrum, a wavelength region of extreme technological interest, may prove to be of tremendous importance for optical applications. In addition, the silver element is the required composition of the resulting core−shell nanoparticles. The nanoparticle-based platform is thus demonstrated to be a highly selective and sensitive nanosensor for silver ions in aqueous media.

EXPERIMENTAL SECTION

Materials. $HAuCl_4 \cdot 3H_2O$, cetyltrimethylammonium bromide (CTAB), $Na_2S_2O_3$, ascorbic acid, and silver nitrate were purchased from Sinopharm Chemical Reagent Co., Ltd. (Shanghai, China). All of the chemicals, unless mentioned otherwise, were of analytical reagent grade and used as received. The aqueous solutions were prepared in doubly distilled water.

Preparation of Gold Nanoparticles. The CTAB solution (1.5 mL, 0.1 M) was mixed with 100 μL of 0.02 M $HAuCl_4$. One hundred microliters of ice-cold 0.01 M $NaBH_4$ was added while the solution was stirred, resulting in the formation of a brownish yellow solution. Vigorous stirring of the solution continued for 4 h at 70 °C. The solution was kept at room temperature (25 °C) and used at least 5 days after preparation.

Preparation of Gold Nanorods (GNRs). The GNRs were prepared according to the seeded growth method without the addition of $AgNO_3$ as reported previously.[30,31] Synthesis of the seed solution is the same as that of the gold nanoparticles mentioned above. The solution was kept at room temperature (25 °C) and used at least 2 h after preparation to produce the GNRs. One and a half milliliters of 0.02 M $HAuCl_4$ was added to 30 mL of 0.1 M CTAB, followed by the addition of 0.8 mL of 0.08 M ascorbic acid. Ascorbic acid here worked as a mild reducing agent and changed the color of the solution from dark yellow to colorless. Finally, 70 μL of the seed solution was added to the solution and the color changed gradually in 30 min.

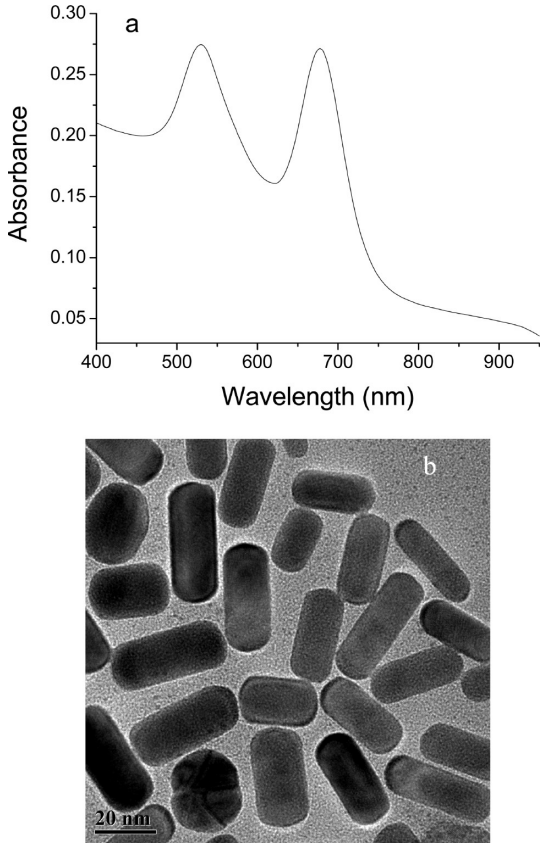

Figure 1. (a) LSPR optical spectrum acquired from the gold nanorods and (b) corresponding TEM image.

Fabrication of Core−Shell Gold Nanoparticles and Determination of Ag^+. A series of different concentration of Ag^+ solution (1×10^{-3}, 1×10^{-4}, 1×10^{-5}, 1×10^{-6}, 1×10^{-7}, 1×10^{-8} M) were detected based on the core−shell technique. Briefly, 50 μL of 0.1 M $Na_2S_2O_3$ and the Ag^+ sample solution were added to 2 mL of the synthesized gold nanoparticles at room temperature, respectively. The LSPR optical results were obtained from the nanorods on a UV−visible spectrophotometer (Lambda 35, Perkin-Elmer). Because the plasmon band of the resulting nanoparticles red-shifted with increasing reaction time, various stages were monitored at different reaction time intervals and the final spectrum was recorded as the signal to detect the Ag^+ concentration.

Characterization. Transmission electron microscopy (TEM) was performed on a JEM-2010 transmission electron microscope at 80 kV. The X-ray diffraction (XRD) data were obtained on a Siemens D5000 diffractometer equipped with the Cu $K_{\alpha 1}$ (λ = 1.54056 Å) X-ray source and analyzed using Traces Software. X-ray photoelectron spectra (XPS) were acquired using ESCALab201i-XL spectrometer (VG Scientific Ltd., East Grinstead, Sussex, U.K.). The base pressure during data acquisition was about 3×10^{-7} Pa. The C1s line (284.6 eV) was used for energy calibration. Energy-dispersive X-ray spectroscopy was conducted at 25 kV on a JEOL JSM-6380LV field-emission scanning electron microscope (FEI Co.).

RESULTS AND DISCUSSION

Preparation of Core−Shell Nanoparticles. A number of methods have been developed to synthesize gold nanorods (GNRs) and the addition of $AgNO_3$ provides some advantages by allowing better control of the shape of the synthesized

GNRs. In this study, in order to investigate the effects of Ag^+ during subsequently fabricating core−shell nanostructure, GNRs prepared without $AgNO_3$ are employed. As previously reported,[32,33] the yield of the nanorods is low because of the existence of abundant spherelike gold nanoparticles. Figure 1a depicts the LSPR optical spectrum with a transverse plasmon wavelength (TPW) at 531 nm and longitudinal plasmon wavelength (LPW) at 678 nm. The high intensity in the transverse plasmon band implies that there are many spherelike gold nanoparticles in the prepared GNRs, as shown in Figure 1b.

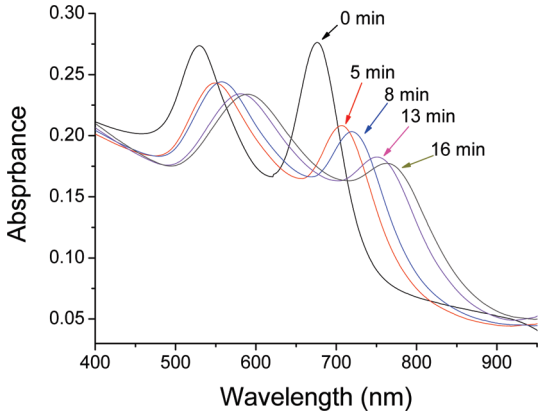

Figure 2. LSPR optical spectra acquired from the GNRs after reacting with $Na_2S_2O_3$ and $AgNO_3$ for different time durations.

The core−shell nanostructured particles are produced by reacting $AgNO_3$ and $Na_2S_2O_3$ with gold nanoparticles in an aqueous solution. In the process of reaction, the reaction system was performed exposing to air. Initially, 50 μL of 0.1 M $Na_2S_2O_3$ is added to the gold nanoparticles suspension (2 mL) and slightly reduced absorption intensity is observed because $Na_2S_2O_3$ is able to etch gold nanoparticles in the solution.[34] With the addition of $AgNO_3$ to the mixed solution, a continuous red shift in the LPW and TPW accompanied by reduced intensity is observed as the reaction progresses. At the same time, the color of the solution changes gradually from wine red to pale green. Figure 2 shows the temporal evolution of the GNRs reacting with $Na_2S_2O_3$ and 1×10^{-4} M $AgNO_3$ at room temperature. This Figure shows that the LPW exhibits a larger change than TPW. With fixed concentrations of GNRs and $Na_2S_2O_3$, the final LPW of the core−shell nanorods depends on the concentration of added Ag^+.

Figure 3a shows X-ray photoelectron spectroscopy (XPS) of the nanorods obtained from GNRs reacting with $Na_2S_2O_3$, demonstrating Au, S, and Ag in these nanoparticles. According to the X-ray diffraction (XRD) patterns in Figure 3b and previous reports, the nanoparticles consist of Au and complex salts, namely Au_2S, AuAgS,[35−39] and Ag_3AuS_2.[40,41] Although these experimental data from XPS and XRD were acquired by averaged over large areas of these nanoparticls, Figure 4 shows two different phases in the formed nanorods indicating the formation of a core−shell structure. Furthermore, high-resolution transmission electron microscopy (HR-TEM) confirms that both the Au core and shell are crystalline. Therefore, the

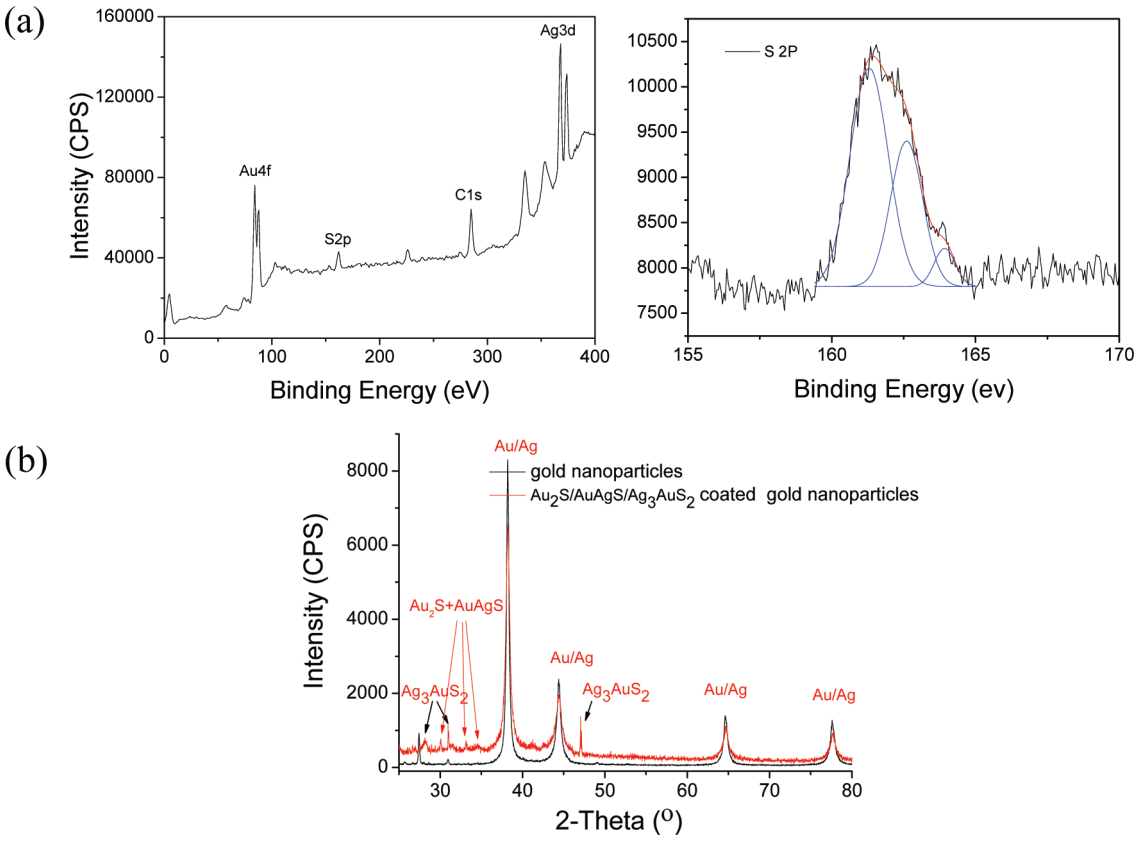

Figure 3. (a) XPS spectra measured from core−shell nanoparticles with peak identity labeled by element symbol. (b) Comparison of the XRD spectra obtained from the gold nanoparticles and formed core−shell nanoparticles (Au_2S/AuAgS/Ag_3AuS_2 coated gold nanoparticles).

dx.doi.org/10.1021/am101034h |ACS Appl. Mater. Interfaces 2011, 3, 183–190

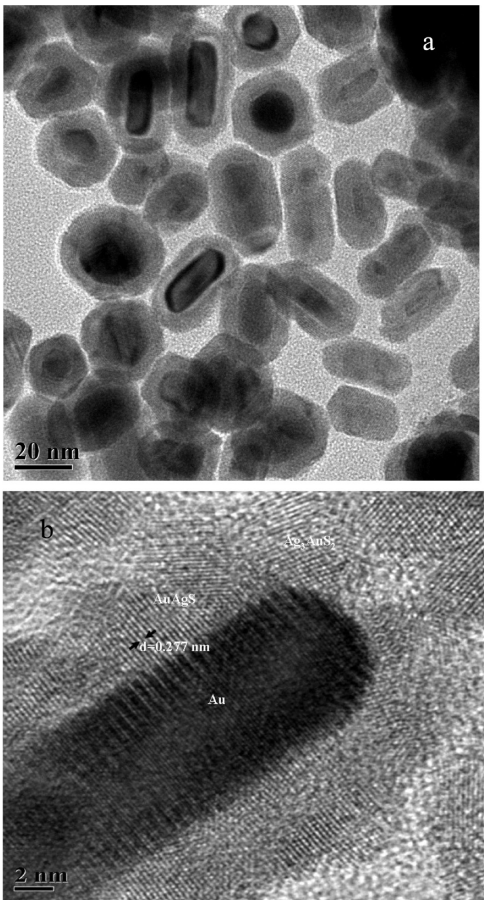

Figure 4. (a)TEM image of the core−shell nanostructure acquired from GNRs reacting with Ag^+ and $Na_2S_2O_3$, (b) HR-TEM image of core−shell nanorods.

two different phases can be ascribed to the chalcogenide layer, Au_2S, AuAgS, and Ag_3AuS_2 covering the GNR, and reduced GNR core. The EDS spectra acquired from the core−shell nanorods at various stages shown in Figure S1 (see the Supporting Information) reveal that the amounts of S and Ag increase with the reaction of gold nanorods with $Na_2S_2O_3$ and Ag^+, further demonstrating that the increasing shell thickness results form the gold nanorods reacting successively with $Na_2S_2O_3$ and Ag^+ to form the chalcogenide layer. Consequently, the core−shell structure of the nanoparticles can be controlled.

Spherelike gold nanoparticles can also form the core−shell structure. With the addition of $Na_2S_2O_3$ and Ag^+, a significant red shift appears in the LSPR optical spectra as shown in Figure 5a. A distinct core−shell structure is revealed in the TEM images in Figure 5b. The metal chalcogenide layer is a narrow band gap semiconductor with a large refractive index at typical optical frequencies. As a result, red shifts in the plasmon peak occur from the larger refractive index chalcogenide layer covering the gold nanoparticles and consequently, plasmon-induced absorption spectra are expected. Furthermore, a continuous red shift in the plasmon peak accompanied by reduced intensity is observed as the reaction proceeds as shown in Figures 2 and 5a. Compared to Figure 3, the layer on the core−shell nanoparticle in Figure 5 shows small change due to the different reaction temperature. It is known that increasing the temperature can significantly enhance the reaction rate. The core−shell structure in Figure 5 is obtained by heating the reaction system to 60 °C, whereas the core−shell nanorods shown in Figure 3 are obtained by a reaction between gold nanorods, $AgNO_3$ and $Na_2S_2O_3$ at room temperature. It is possible that the ratio of these components can vary slightly at different reaction temperature, but the core−shell nanoparticles produced from the gold nanoparticles by the two aforementioned methods have the similar characteristics.

Preparation of Different Size Core−Shell Nanoparticles. $S_2O_3^{2-}$ can form soluble complex compounds with many metal ions such as Au^{3+}, Ag^+, Cu^{2+}, Cd^{2+}, and so on. As aforementioned, with the addition of $Na_2S_2O_3$ and $AgNO_3$, a red shift in the plasmon peak is observed from the nanoparticles. However, if only $Na_2S_2O_3$ is added to the GNR suspension, a slight blue shift in lieu of a red shift is observed from the plasmon peak and the absorption intensity diminishes gradually as shown in Figure 6a. Similarly, decreasing absorption intensity is found after the spherelike nanoparticles react with $Na_2S_2O_3$ (Figure 6b). The results suggest that the gold atoms on the surface of the nanoparticles can react with $Na_2S_2O_3$ to generate a soluble complex $Au(S_2O_3)_2^{3-}$ thereby changing the nanoparticle size. As a result, nanoparticles with a much smaller size form as the nanoparticles are etched by $Na_2S_2O_3$ shown in Figure S2 in the Supporting Information. Therefore, gold nanoparticles with different sizes can be produced by varying the reaction conditions such as the concentration and reaction time. Interestingly, subsequent addition of a trace quantity of Ag^+ can produce a red shift in the plasmon peak due to the formation of a layer of Au_2S/AuAgS/Ag_3AuS_2 on the gold nanoparticles. The TEM image shows that the core−shell nanoparticles with controllable shell thickness are produced (Figure 7) and similarly, smaller core−shell nanoparticles can be generated in a controlled fashion.

In this technique, the chemical reactions that produce the signal changes stabilize within 30 min at room temperature and heating can significantly decrease the response time. If $Na_2S_2O_3$ is added to the gold nanoparticles suspension, Au can react with it to produce a soluble complex compound, and finally the gold colloid disappears. However, with the addition of $Na_2S_2O_3$ and $AgNO_3$ to the gold nanoparticles, the complex salts Au_2S, AuAgS, and Ag_3AuS_2 are generated to cover the gold nanoparticles. The chemical reactions that arise on the surface of gold nanoparticles are also illustrated in Scheme 1 are described as follows (first reaction from ref 42)

$$4Au + O_2 + 8S_2O_3^{2-} + 2H_2O \rightarrow 4Au(S_2O_3)_2^{3-} + 4OH^-$$

$$3Au(S_2O_3)_2^{3-} + Ag^+ + 6H_2O + 2H^+ \rightarrow Au_2S + AuAgS + 6HSO_4^- + 4H_2S$$

$$Au(S_2O_3)_2^{3-} + 3Ag^+ + 2H_2O \rightarrow Ag_3AuS_2 + 2HSO_4^- + 2H^+$$

This shell technique produces insoluble complex salts comprising Au_2S, AuAgS, and Ag_3AuS_2, and then the shell surrounding the gold nanoparticle is formed. However, our experimental results indicate that this process converts Au atoms into Au_2S AuAgS, and Ag_3AuS_2. Similarly, our previous work shows the GNRs might react with Na_2S to produce Au_2S/AuAgS-coated

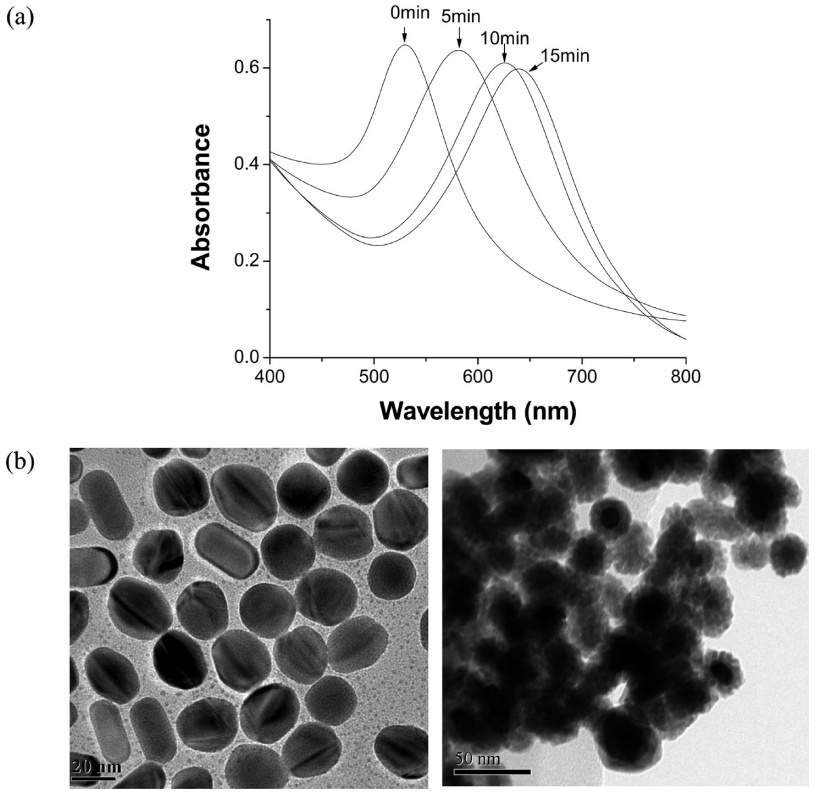

Figure 5. (a) LSPR optical spectra acquired from the gold nanospheres after reacting with $Na_2S_2O_3$ and Ag^+ for different time durations. (b) TEM images of the gold nanoparticles and resulting core−shell nanostructures after reacting the gold nanoparticles with $AgNO_3$ and $Na_2S_2O_3$.

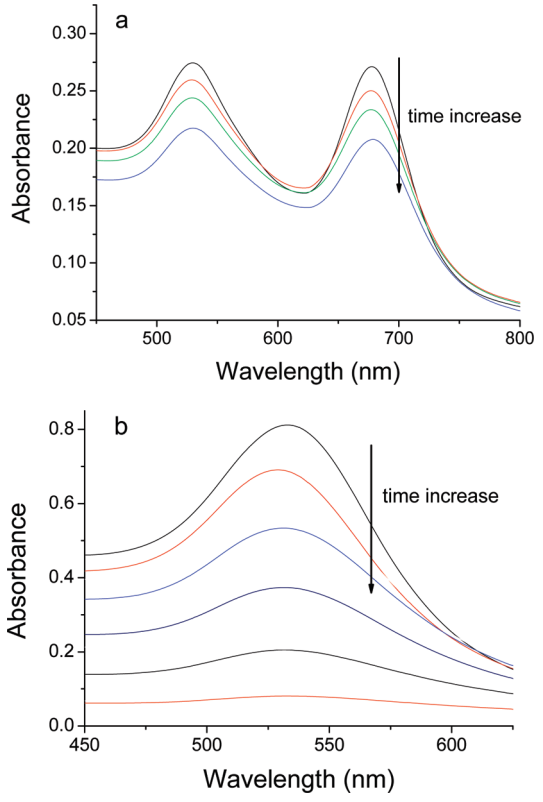

Figure 6. Optical spectra of (a) gold nanorods and (b) spherelike gold nanoparticles after reacting with $Na_2S_2O_3$ (time duration: 5 min).

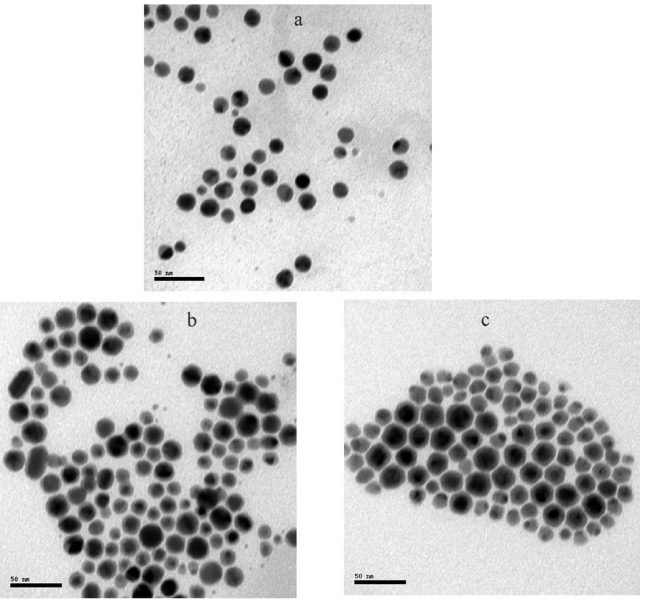

Figure 7. TEM images elucidate evolution of the core−shell gold nanosphere based on as-prepared gold nanosphere, (a) represents as-prepared gold nanosphere (absorption peak: 520 nm), (b) core−shell gold nanosphere with absorption peak is 590 nm, (c) core−shell gold nanosphere with absorption peak is 660 nm.

gold nanorods.[35] HR-TEM and XRD demonstrate that they have the similar core−shell nanostructure and components. Although the two approaches use different reactions in the formation of

Scheme 1. Schematic Illustration of Changes in the Gold Nanoparticles and Formation of Core-Shell Nanoparticles under Different Conditions

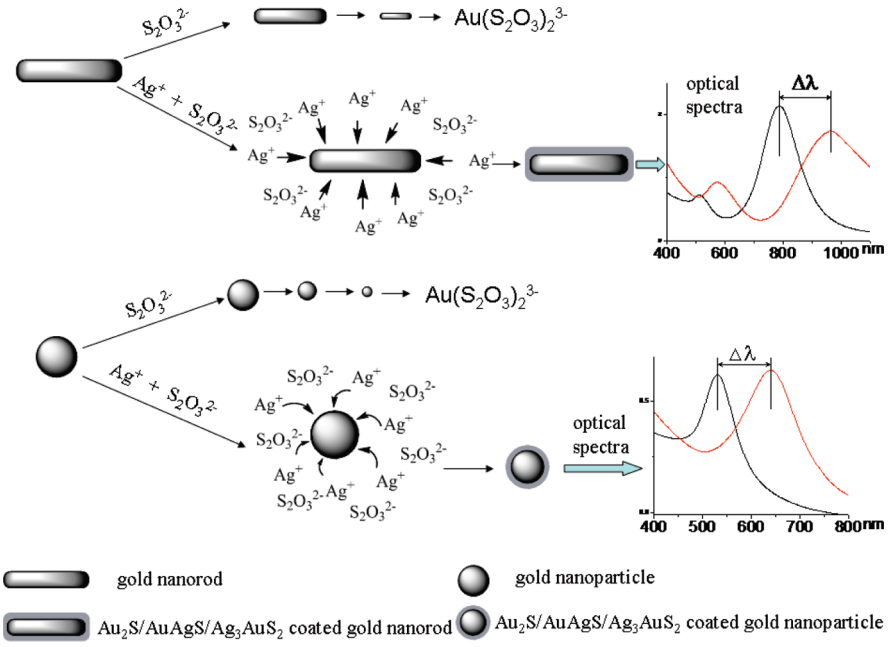

complex salts consisting of Au_2S, AuAgS, and Ag_3AuS_2, formation of the Au_2S, AuAgS, and Ag_3AuS_2 shell occurs from the outside. Obviously, the morphological evolution of the particles changes significantly with reaction time in a way dominated by diffusion processes, as shown in Figure 8. A layer of shell, Au_2S, AuAgS, and Ag_3AuS_2, is formed with the Ag^+ and $S_2O_3^{2-}$ reacting with Au followed by diffusion of Ag^+ and S^{2-} in the solid of the Au_2S/AuAgS/Ag_3AuS_2-coated gold nanoparticles to generate Au_2S, AuAgS, and Ag_3AuS_2 sequentially. Generally, increasing temperature can lead to the increment of reaction rate. With increasing temperature, it is possible that a significantly enhanced diffusion rate increases the thickness of the shell. In addition, previous works has been demonstrated that the Ag^+ and S^{2-} could diffuse in the solid states.[43−46] As a result, a significant enhancement of red shift in the plasmon wavelength appears as the increase of temperature. Simultaneous existence of the two species ($AgNO_3$ and $Na_2S_2O_3$) in the solution is necessary for diffusion to take place in the Au_2S/AuAgS-coated gold nanoparticles. Although the sulfide ion can react with Au to yield Au_2S, there is no change in the plasmon wavelength when the core−shell nanoparticles and $Na_2S_2O_3$ are mixed for 15 days at room temperature as demonstrated by TEM (not shown here). Similarly, there is no detectable change in the plasmon wavelength when the core shell nanoparticles are mixed with $AgNO_3$.

Detection of Ag^+ Based on the Core−Shell Technique. According to the above discussion, the added Ag^+ plays a key role in the formation of the core−shell nanostructure. In fact, addition of a trace amount of Ag^+ to the solution of gold nanoparticles and $Na_2S_2O_3$ can lead to a significant red shift in the plasmon wavelength due to the formation of Au_2S/AuAgS/Ag_3AuS_2 and this forms the basis for detection of Ag^+. Hence, detection of Ag^+ in aqueous media by these gold nanoparticles is possible. A series of solution with different concentrations of Ag^+ react with the gold nanoparticles and the results show that 1×10^{-8} M of Ag^+ can be detected. At the same time, the EDS results show that the atomic content of Ag in the core−shell nanostructure is around 5%.

The selectivity of this system for Ag^+ is evaluated by comparing the responses to other metal ions such as Cu^{2+}, Co^{2+}, Ni^{2+}, Pb^{2+}, Hg^{2+} Cd^{2+}, Zn^{2+}, Fe^{3+}, and Al^{3+} at a concentration of 1×10^{-2} M. Cu^{2+} also leads to a red shift in the plasmon peak in spite of the reduced signal compared to Ag^+. In addition, only a higher concentration of Co^{2+} and Ni^{2+} ($>1 \times 10^{-2}$ M) can lead to a slight red shift of the plasmon peaks, and no noticeable plasmon peak wavelength changes is found at concentrations less than 1×10^{-4} M. That is, interferences by Co^{2+} and Ni^{2+} can be neglect at low concentrations. The other ions investigated here hardly show any effects on the plasmon peak wavelength implying that most of these metal ions cannot form complex salts with Au in the shell layer on the gold nanoparticles.

To further improve the selectivity of this system and eliminate possible interferences from Cu^{2+}, Co^{2+}, and Ni^{2+}, a chelating agent ethylene diamine tetraacetic acid (EDTA) which can form strong complexes with many metal ions can be used. As shown in Figure 9, EDTA can mask the interfering ions with the exception of Ag^+ and consequently, silver ions can be detected with high selectively. Moreover, in order to evaluate the sensitivity of this system, two types of nanoparticles with the same concentration react with the same amount of Ag^+. A comparison of the results obtained from gold nanorods and gold nanosphere shows different response to Ag^+. As reported previously,[47] the LPWs of GNRs are highly sensitive to changes in the dielectric properties of the surroundings and the sensitivity increases with the aspect ratio of GNRs. Generally, the aspect ratio of gold nanosphere is 1 and that of GNRs is larger than 1. As a result, the GNRs are more sensitive than gold nanospheres and the response from various concentrations of Ag^+ by GNRs is displayed in Figure 10. In this process of detecting Ag^+ concentration, when the absorption intensity of the gold nanorods was fixed around

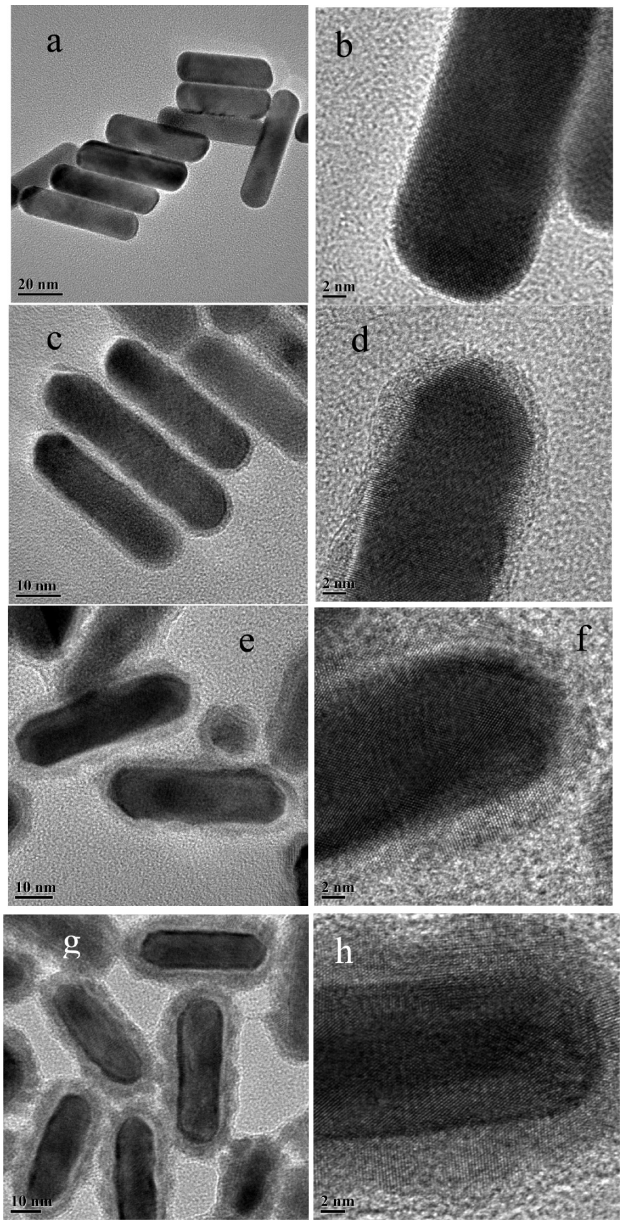

Figure 8. (a, c, e, g) TEM and the related (b, d, f, h) HRTEM images of nanorods changes acquired by the synthesized gold nanorods (a) reacting with $Na_2S_2O_3$ and Ag^+ at different reaction time. The thickness of the shell of these resulting core−shell nanorods (b−d) is 2, 4, and 7 nm, respectively.

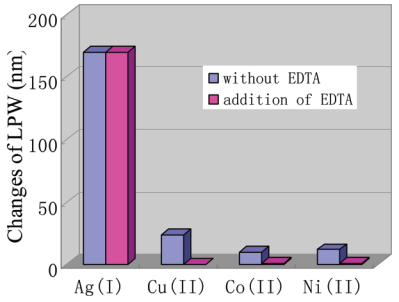

Figure 9. Changes in the longitudinal plasmon wavelengths observed from the gold nanoparticles after reacting with 1×10^{-2} M of different metal ions before and after the addition of chelating agent EDTA.

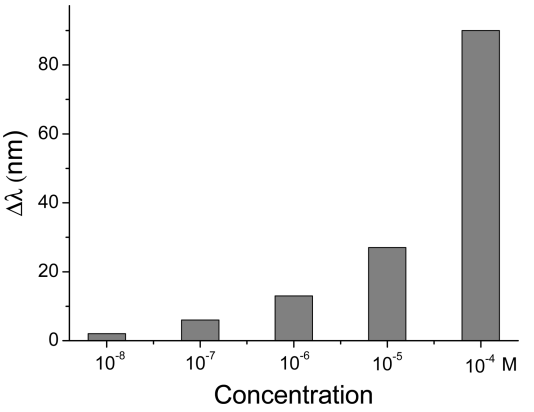

Figure 10. LPW changes obtained from GNRs after reacting with different concentrations of Ag^+.

0.12, our results show that Ag^+ concentrations as small as 1×10^{-8} M can be detected by this method.

CONCLUSION

A novel shell technique to fabricate controllable core−shell nanoparticles has been developed. $Na_2S_2O_3$ can etch gold nanoparticles and produces nanoparticles with different sizes. However, the special reaction indicates that addition of Ag^+ to the gold nanorod and $Na_2S_2O_3$ suspension not only prevents the etching reaction but also leads to the formation of Au_2S/AuAgS/Ag_3AuS_2-coated gold nanoparticles. Therefore, gold nanoparticles and Au_2S/AuAgS/Ag_3AuS_2-coated gold nanorods with variable sizes can be formed. Both the shell thickness and core size can be controlled during the formation of the core−shell nanoparticles. Moreover, a nanosensing platform incorporating core−shell gold nanoparticles synthesized by this technique is demonstrated and Ag^+ can be detected with remarkably high selectivity and sensitivity.

ASSOCIATED CONTENT

Supporting Information. EDS spectra of GNRs and the resulting core−shell nanorods obtained by the GNRs reacting with $Na_2S_2O_3$ and $AgNO_3$ at different stages. This material is available free of charge via the Internet at http://pubs.acs.org/.

AUTHOR INFORMATION

Corresponding Author
*hhwn09@163.com (H.H.); paul.chu@cityu.edu.hk (P.K.C.).

ACKNOWLEDGMENT

This work was jointly supported by Natural Science Foundation of China (21075035), Hunan Provincial Natural Science Foundation of China (10JJ5004), National Basic Research Fund (2005CB623901), Shanghai Science and Technology R&D Fund (0952 nm04400, 0852 nm03300, 07JC14057), and Hong Kong Research Grants Council (RGC) General Research Funds (GRF) CityU 112307.

REFERENCES

(1) Sardar, R.; Funston, A. M.; Mulvaney, P.; Murray, R. W. *Langmuir* **2009**, *25*, 13840–13851.

(2) Harpeness, R.; Gedanken, A. *Langmuir* **2004**, *20*, 3431–3434.
(3) Burda, C.; Chen, X.; Narayanan, R.; El-Sayed, M. A. *Chem. Rev.* **2005**, *105*, 1025–1102.
(4) Okuno, Y.; Nishioka, K.; Kiya, A.; Nakashima, N.; Ishibashi, A.; Niidome, Y. *Nanoscale* **2010**, *2*, 1489–1493.
(5) Wang, H.; Brandl, D. W.; Nordlander, P.; Halas, N. J. *Acc. Chem. Res.* **2007**, *40*, 53–62.
(6) Xie, W.; Su, L.; Donfack, P.; Shen, A.; Zhou, X.; Sackmann, M.; Materny, A.; Hu, J. *Chem. Commun.* **2009**, 5263–5265.
(7) Hodak, J. A.; Henglein, A.; Hartland, G. V. *J. Phys. Chem. B* **2000**, *104*, 11708–11718.
(8) Panigrahi, S.; Praharaj, S.; Basu, S.; Ghosh, S. K.; Jana, S.; Pande, S.; Vo-Dinh, T.; Jiang, H.; Pal, T. *J. Phys. Chem. B* **2006**, *110*, 13436–13444.
(9) Jackson, J. B.; Halas, N. J. *J. Phys. Chem. B* **2001**, *105*, 2743–2746.
(10) Mulvaney, P.; Giersig, M.; Henglein, A. *J. Phys. Chem.* **1993**, *97*, 7061–7064.
(11) Doering, W. E.; Piotti, M. E.; Natan, M. J. *Adv. Mater.* **2007**, *19*, 3100–3108.
(12) Wu, C.; Xu, Q. H. *Langmuir* **2009**, *25*, 9441–9446.
(13) Ming, T.; Zhao, L.; Yang, Z.; Chen, H. J.; Sun, L. D.; Wang, J. F.; Yan, C. H. *Nano Lett.* **2009**, *9*, 3896–3903.
(14) Wanjala, B. N.; Luo, J.; Loukrakpam, R.; Fang, B.; Mott, D.; Njoki, P. N.; Engelhard, M.; Naslund, H. R.; Wu, J. K.; Wang, L.; Malis, O.; Zhong, C. J. *Chem. Mater.* **2010**, *22*, 4282–4294.
(15) Lu, L.; Wang, H.; Zhou, Y.; Xi, S.; Zhang, H.; Hu, J.; Zhao, B. *Chem. Commun.* **2002**, 144–145.
(16) Neretina, S.; Dreaden, E. C.; Qian, W.; El-Sayed, M. A.; Hughes, R. A.; Preston, J. S.; Mascher, P. *Nano Lett.* **2009**, *9*, 3772–3779.
(17) Ni, W. H.; Chen, H. J.; Su, J.; Sun, Z. H.; Wang, J. F.; Wu, H. K. *J. Am. Chem. Soc.* **2010**, *132*, 4806–4814.
(18) Liang, C. H.; Wang, C. C.; Lin, Y. C.; Chen, C. H.; Wong, C. H.; Wu, C. Y. *Anal. Chem.* **2009**, *81*, 7750–7756.
(19) Kumagai, M.; Sarma, T. K.; Cabral, H.; Kaida, S.; Sekino, M.; Herlambang, N.; Osada, K.; Kano, M. R.; Nishiyama, N.; Kataoka, K. *Macromol. Rapid Comm.* **2010**, *31*, 1521–1528.
(20) Wang, L.; Park, H. Y.; Lim, S. I. I.; Schadt, M. J.; Mott, D.; Luo, J.; Wang, X.; Zhong, C. J. *J. Mater. Chem.* **2008**, *18*, 2629–2635.
(21) Li, D.; Wieckowska, A.; Willner, I. *Angew. Chem., Int. Ed.* **2008**, *47*, 3927–3931.
(22) Liu, J.; Lu, Y. *J. Am. Chem. Soc.* **2004**, *126*, 12298–12305.
(23) Kim, Y.; Johnson, R. C.; Hupp, J. T. *Nano Lett.* **2001**, *1*, 165–167.
(24) Arduini, M.; Mancin, F.; Tecilla, P.; Tonellato, U. *Langmuir* **2007**, *23*, 8632–8636.
(25) Yin, J.; Guan, X.; Wang, D.; Liu, S. *Langmuir* **2009**, *25*, 11367–11374.
(26) Zhou, H. S.; Honma, I.; Komiyama, H.; Haus, J. W. *Phys. Rev. B* **1994**, *16*, 12052–12056.
(27) Averitt, R. D.; Sarkar, D.; Halas, N. J. *Phys. Rev. Lett.* **1997**, *78*, 4217–4220.
(28) Liu, M.; Guyot-Sionnest, P. J. *Mater. Chem.* **2006**, *16*, 3942–3945.
(29) Bao, Z. H.; Sun, Z. H.; Xiao, M. D.; Tian, L. W.; Wang, J. F. *Nanoscale* **2010**, *2*, 1650–1652.
(30) Jana, N. R.; Gearheart, L.; Murphy, C. J. *J. Phys. Chem. B* **2001**, *105*, 4065–4067.
(31) Busbee, B. D.; Obare, S. O.; Murphy, C. J. *Adv. Mater.* **2003**, *15*, 414–416.
(32) Jana, N. R.; Gearheart, L.; Murphy, C. J. *J. Phys. Chem. B* **2001**, *105*, 4065–4067.
(33) Pérez-Juste, J.; Liz-Marzán, L. M.; Carnie, S.; Chan, D. Y. C.; Mulvaney, P. *Adv. Funct. Mater.* **2004**, *14*, 571–579.
(34) Zhang, X. M.; Senanayake, G.; Nicol, M. J. *Hydrometallurgy* **2004**, *74*, 243–257.
(35) Huang, H.; Liu, X.; Zeng, Y.; Yu, X.; Liao, B.; Yi, P.; Chu, P. K. *Biomaterials* **2009**, *30*, 5622–5630.
(36) Ishikawa, K.; Isonaga, T.; Wakita, S.; Suzuki, Y. *Solid State Ionics* **1995**, *79*, 60–66.
(37) Gurevich, V. M.; Gavrichev, K. S.; Gorbunov, V. E.; Baranova, N. N.; Tagirov, B. R.; Golushina, L. N.; Polyakov, V. B. *Thermochim. Acta* **2004**, *412*, 85–90.
(38) Osadchii, E. G.; Rappo, O. A. *Am. Mineral.* **2004**, *89*, 1405–1410.
(39) Zhai, H. J.; Bürgel, C.; Bonacic-Koutecky, V.; Wang, L. S. *J. Am. Chem. Soc.* **2008**, *130*, 9156–9167.
(40) Sakai, H.; Ando, M.; Ichiba, S.; Maeda, Y. *Chem. Lett.* **1991**, 223–226.
(41) Smit, T. J. M.; Venema, E.; Wiersma, J.; Wiegers, G. A. *J. Solid State Chem.* **1970**, *2*, 309–312.
(42) Aylmore, M. G.; Muir, D. M. *Miner. Eng.* **2001**, *14*, 135–174.
(43) Hodak, J. H.; Henglein, A.; Hartland, G. V. *J. Phys. Chem. B* **2000**, *104*, 11708–11718.
(44) Yin, Y.; Erdonmez, C. K.; Cabot, A.; Hughes, S.; Alivisatos, A. P. *Adv. Funct. Mater.* **2006**, *16*, 1389–1399.
(45) Drugov, Y.; Tsegelnik, V.; Bolotov, A.; Vlasov, Y.; Bychkov, E. *Solid State Ionics* **2000**, *136−137*, 1091–1096.
(46) Macková, A.; Švorčík, V.; Strýhal, Z.; Pavlík, J. *Surf. Interface Anal.* **2006**, *38*, 335–338.
(47) Yang, D. P.; Cui, D. X. *Chem. Asian J.* **2008**, *3*, 2010–2022.